Performance and Plume Characterization of the BHT-1500 Hall Thruster

IEPC-2015-69／ISTS-2015-b-69

Presented at Joint Conference of 30th International Symposium on Space Technology and Science
34th International Electric Propulsion Conference and 6th Nano-satellite Symposium,
Hyogo-Kobe, Japan
July 4 – 10, 2015

Kevin D. Diamant,[1] Thomas J. Curtiss,[2] Rostislav Spektor,[3] and Edward J. Beiting[4]
The Aerospace Corporation, El Segundo, CA, 90245, USA

Vlad Hruby,[5] Bruce Pote,[6] Juraj Kolencik,[7] and Surjeet Paintal[8]
Busek Company, Inc., Natick, MA, 01760, USA

The BHT-1500 Hall thruster was characterized with respect to performance and angle-dependent plume properties at discharge powers of 1.5 and 1.8 kW and discharge voltages of 300 and 400 V over vacuum chamber background pressures ranging from 2.9E-6 to 4.1E-5 Torr. The thruster was operated with an externally as well as an internally mounted cathode. Operation with the internally mounted cathode conferred a number of advantages, including improved performance, reduced sensitivity of performance to cathode flow rate, more efficient cathode-plume coupling, and reduced sensitivity of the aforementioned, as well as plume divergence, to vacuum facility background pressure. Other parameters, including discharge oscillations, the most probable primary ion energy-to-charge ratio, the fraction of multi-charged ions, and the total xenon flow rate were found to vary with background pressure in ways that were largely unaffected by cathode location.

I. Introduction

THE BHT-1500 single-stage Hall thruster was created at Busek Company, Inc. (Busek) and incorporates design features, such as a two-piece "composite" anode and shortened dielectric channel,[1,2] that distinguish it from SPT-type designs. In the work described here, the thruster was operated at The Aerospace Corporation (Aerospace) at discharge powers of 1.5 and 1.8 kW and discharge voltages of 300 and 400 V with both externally and internally mounted cathodes. The internally mounted cathode was on thruster centerline. This paper presents measurements of thruster performance and plume properties (angle-dependent ion flux, energy, and charge-state distributions, and plasma potentials, densities, and electron temperatures) as functions of cathode location and vacuum chamber background pressure (from 2.9E-6 to 4.1E-5 Torr).

II. Experimental Apparatus

A. Busek BHT-1500 Hall thruster

[1] Research Scientist, Propulsion Science, kevin.d.diamant@aero.org.
[2] Department Director, Propulsion Science, thomas.j.curtiss@aero.org.
[3] Laboratory Manager, Propulsion Science, rostislav.spektor@aero.org.
[4] Senior Scientist, Propulsion Science, edward.j.beiting@aero.org.
[5] President, vhruby@busek.com.
[6] Director, Hall Thrusters, bpote@busek.com.
[7] Research Engineer, george@busek.com.
[8] Research Engineer, spaintal@busek.com.

Figure 1 shows the thruster installed in the Aerospace vacuum chamber. The baseline thruster design incorporates the internally mounted cathode. The external cathode was included for information only. The ceramic exit rings were pre-machined to a shape representative of 8000 hours of wear. The BHT-1500 uses one centrally mounted electromagnet coil and 4 outer electromagnet coils whose axes are not coincident with thruster centerline. In this configuration, the magnetic field has a separatrix located off of the thruster axis, i.e., a surface downstream of the thruster exit plane where the curvature of magnetic field lines changes from bending toward thruster centerline to bending away from it. The thruster is shown operating with each cathode in Fig. 2. At high background pressure (4.0E-5 Torr), a visible plume extended from the external cathode away from thruster centerline, presumably indicating that the cathode exit aperture was located outside of the separatrix. At lower background pressure, the external cathode plume was only visible for a short distance. It is likely that electrons emitted by the external cathode still followed magnetic field lines away from thruster centerline at low pressure, but there were not enough background neutrals available to be excited by electron impact to create an extended visible plume.

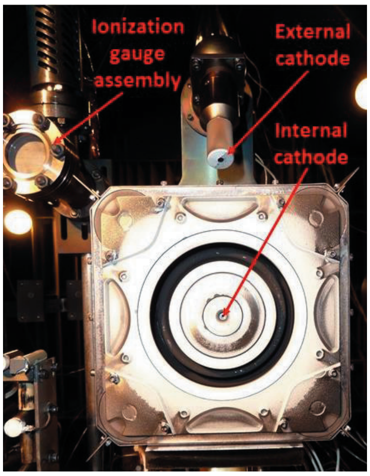

Figure 1. BHT-1500 installed in the vacuum test facility at The Aerospace Corporation.

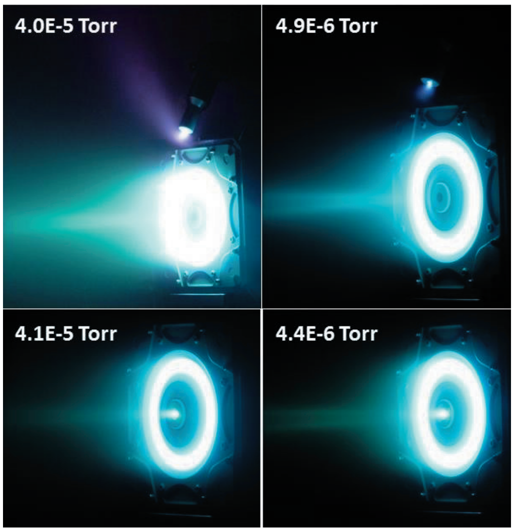

Figure 2. BHT-1500 operating at 1.8kW, 300 V at high and low background pressure with external cathode (top panels) and internal cathode (bottom panels).

B. Vacuum facility

The Aerospace vacuum facility is a 2.4 m diameter by 9.8 m long cryopumped vacuum chamber with a maximum measured xenon pumping speed of approximately 250 kl/s. Vacuum facility background pressures were measured with an internally mounted, metal-encapsulated “Stabil-ion” ionization gauge. The gauge was mounted on a 2-3/4 inch conflat “tee” so that ingested plasma would have to make a right-angle turn, and presumably be neutralized by wall collisions, before reaching the gauge. The entrance aperture to the tee was equipped with two wire-mesh grids with approximately 25 μm apertures and open area fraction of 38%. The first grid could be biased to repel electrons, and the second to repel ions, however it was found experimentally that grid biasing affected pressure readings by approximately 1% relative to the unbiased case, and so the grids were left floating. The gauge was calibrated in air against a NIST-traceable standard (spinning rotor gauge), and was found to differ from the standard by 5% or less over the range of pressures reported here. The gauge was mounted with the tee entrance aperture facing in the same direction as the thruster exit plane. This orientation ensured that directed neutral flux, such as could arise from a pressure gradient in the vacuum chamber, would enter the gauge as it would the thruster. The centerline of the tee entrance aperture was located 20 cm radially from thruster centerline at approximately the 10 o'clock position when facing the thruster exit plane, and the plane of the entrance aperture was 10 cm behind the thruster exit plane (Fig. 1).

Vacuum chamber background pressure was varied through a combination of varying the number of active pumps and by injecting excess xenon. Excess xenon was injected through a port located on the chamber wall at chamber centerline and approximately 1.4 m downstream of the thruster exit plane.

Ionization gauge readings were corrected using the scale factor of 0.348 specified by the gauge manufacturer for xenon relative to nitrogen.

C. Thruster operation

The BHT-1500 was operated at fixed discharge voltages of 300 and 400 V at each power level (1.5 and 1.8 kW) with laboratory power supplies and xenon flow controllers. A discharge filter consisting of a 23.0 μF capacitor was connected across the terminals of the discharge supply. The cathode flow rate was adjusted to maintain a cathode-to-anode flow rate ratio (cathode flow fraction) of 6%, unless otherwise stated. At each operating point, as background pressure or cathode flow fraction was varied the total xenon flow rate was adjusted to maintain the nominal discharge current (e.g., 6.00 A at 300 V, 1.8 kW) to within a variation of 10 mA. The mass flow controllers were calibrated just prior to the test campaign by timing the rate of pressure rise while flowing into a one-liter fixed volume.

The Aerospace vacuum chamber is connected to a dedicated facility ground. The thruster mounting structure and thrust stand were electrically connected to the vacuum chamber.

D. Diagnostics

1. Thrust stand

The thruster was mounted on an inverted-pendulum style thrust stand equipped with load cells for direct thrust measurement. Additional information regarding the thrust stand can be found in Ref. 3. In order to minimize error associated with thermally-induced "zero drift," thrust was measured by recording the difference between thrust sensor outputs with the thruster on and off. That is, the thruster was shut down (no power or propellant flow) and the thrust stand "zero" was checked for every thrust measurement. Also, the thrust stand was calibrated following every measurement. Typically, 2 or 3 measurements were taken at each operating condition and averaged to produce the results reported here. An exception to the preceding statements occurred when we measured the effect of cathode flow fraction on thruster performance. During that study we recorded differences in thrust stand output as cathode flow fraction was varied in stepwise fashion. These differences were joined with absolute measurements taken with the nominal 6% flow fraction to produce the results reported here.

2. Discharge current

Discharge current time histories were recorded with an oscilloscope at a sampling frequency of 500 kHz with a total recording period of 20 ms, corresponding to a Nyquist frequency of 250 kHz and frequency resolution of 25 Hz. The current probe was located outside the vacuum chamber on the anode line on the thruster side of the discharge filter. Values of "discharge current noise" reported here represent the ratio of the standard deviation of the current to its average value.

3. Langmuir probe

Angular surveys of plasma potential, electron temperature, electron density, and ion flux were recorded at a radius of 100 cm from the center of the thruster exit plane using a single-electrode, planar Langmuir probe consisting of a 1.35 cm diameter Kovar collector press fit into the end of a ceramic tube. Angles listed in plots are with respect to thruster centerline (this is the case for the other plume probes as well). Current was recorded as the probe voltage was swept from -20 V to 20 V relative to ground in increments of 0.2 V. Plasma potential was identified as the voltage at which the slope of the current-voltage (I-V) curve attained its maximum value. The ion current collected at plasma potential was estimated by generating a linear fit to the ion-saturation portion of the I-V curve, and extrapolating to plasma potential. In principle, at plasma potential there is no Debye-scale sheath between the probe and the plasma, and the effective probe collector area can be assumed to be equal to the collector geometric area, increasing the accuracy of the estimated ion flux. Electron current vs. voltage at or below plasma potential was obtained by subtracting the estimated ion current (from the linear fit) from the total current. Electron temperature was derived from the slope of a semi-logarithmic plot of the electron I-V curve, and electron density was obtained from the electron current measured at plasma potential using the following expression:

$$n_e = \frac{I_{eo}}{q^{3/2} A} \left(\frac{2\pi m_e}{T_e} \right)^{1/2} \quad (1)$$

where n_e is the electron density, I_{eo} is the electron current at plasma potential, q is the elementary charge, A is the geometric probe collection area, m_e is the electron mass, and T_e is the electron temperature in eV.

4. Retarding potential analyzer

A retarding potential analyzer (RPA) was used to measure ion flux and energy distributions at a radius of 100 cm from the center of the thruster exit plane. Information regarding the RPA design can be found in Ref. 3. Ion flux measurements were made by biasing the ion repelling grid from -20 to 100 V relative to ground in 20 V increments at each angular location. The RPA employed three mesh grids of unknown and time-varying ion transparency, so the effective collection area of the RPA was determined for each data set as the value that would minimize the sum of the squares of the differences between the RPA flux measurements at -20 V and the Langmuir flux data at plasma potential (Section II.D.3.).

For measurements of the ion energy distribution, the repelling grid bias was varied from 0 to 400 V relative to ground in 2 V increments.

5. Ion charge state analyzer

Ion charge state current fractions were measured using the ExB probe described in Ref. 4. The entrance collimator restricted the field of view of the probe to a spot of approximately 1 cm in diameter at the thruster. The probe was aligned on the discharge channel centerline (not the thruster centerline, as was the case with the Langmuir probe and RPA), at a radius of 49 cm from the exit plane. Prior to recording data at each angular location with respect to channel centerline, the probe was rotated about a vertical axis passing through the probe's entrance aperture until the signal from Xe^+ was maximized. This latter angle was typically between 0 and ±2°, meaning that in some instances the probe did not have a direct line of sight to any part of the discharge channel.

Reid et al.[5] recommended weighting current fractions measured with the ExB probe with current density measurements when integrating over angles to determine plume-averaged current fractions. Adoption of this procedure implies that the fraction of ions detectable by the highly collimating ExB probe at a given angle varies with angle, thereby requiring a second probe with wider angular acceptance to produce the weighting factors. Since in our case the source volume was not well known (as mentioned above, in some cases the discharge channel was not even in the field of view of the probe), we chose to integrate the ExB data without weighting factors. We also adopted the simplest method for determining local current fractions, which was to assume that the current due to each charge state was equal to the maximum of its corresponding peak in the ExB probe spectrum.[6]

Charge exchange cross sections for xenon ions with xenon neutrals decrease with increasing charge state, resulting in an increase in the current densities of primary multi-charged ions relative to Xe^+ with distance from the thruster. Charge state fractions presented here have been corrected by assuming only symmetric charge exchange reactions (i.e., $Xe^{n+} + Xe \rightarrow Xe + Xe^{n+}$) with a uniform background of room-temperature neutrals at pressures reported by the ionization gauge. Cross sections were obtained from Ref. 7 (Xe^+ and Xe^{2+}) and Ref. 6 (Xe^{3+}). We were not able to find the relevant cross section for Xe^{4+}, so those data are uncorrected. This is not expected to introduce significant error since the amount of Xe^{4+} was relatively small, and the cross section is probably also quite small.

III. Results

A. Performance and discharge stability

Thrust F, xenon mass flow rate $\dot{m}$, specific impulse I_{sp}, efficiency η, and discharge current time histories were measured as functions of background pressure and cathode flow fraction at the various nominal discharge powers and voltages. Specific impulse and efficiency are defined as:

$$I_{sp} = \frac{F}{\dot{m}g} \tag{2}$$

$$\eta = \frac{F^2}{2\dot{m}(J_D V_D + P_{mag})} \tag{3}$$

where g is Earth's sea-level gravitational acceleration, J_D is the discharge current, V_D is the discharge voltage, and P_{mag} is the magnet power.

Thrust measurement uncertainty was dominated by the repeatability of thrust stand calibrations, and was estimated to be 0.6%. Xenon mass flow rate measurement uncertainty was estimated to be 0.8%. We adopted the conservative approach of summing the uncertainties of each parameter in a product or quotient to obtain estimated uncertainties of 1.4% and 2.0% for specific impulse and efficiency respectively.

1. Nominal cathode flow fraction

Figure 3 presents results obtained as a function of background pressure while operating with the nominal cathode flow fraction of 6%. Thrust varied weakly with background pressure, with tendencies (at least at pressures below 1E-5 Torr) to trend slightly upward with decreasing pressure for operation with the internal cathode, and downward with the external. Similar trends were reported by Hofer and Anderson while operating a 6 kW magnetically shielded Hall thruster with internally and externally mounted cathodes.[8] On average, BHT-1500 thrust was 3.4% larger with the internal cathode than with the external.

With one exception (1.5 kW, 400 V at 4E-5 Torr), the total xenon mass flow rate was, to within measurement uncertainty, the same while operating with either cathode. On average, the mass flow rate increased by 3.6% at the lowest background pressure relative to the highest. This value may be compared to the calculated rate of ingestion from the vacuum chamber, which, based on free molecular flow through the exit plane at the pressure measured by the ionization gauge and an assumed background neutral temperature of 300 K, was at most 1.1% of the flow rate supplied to the anode at the highest background pressure (0.1% at the lowest). If we wish to apply the "simple ingestion" model, whereby propellant entrained from the vacuum chamber is treated as equivalent to propellant supplied to the thruster through the anode, it is necessary to assume an effective ingestion area approximately 3 times larger than the exit plane area to account for the observed variation in flow rate. This idea, however, presumes that the flow ingested through some boundary that extends well beyond the exit plane is ionized and accelerated in the same manner as if it had been supplied through the anode, which is unlikely to be true. In fact, as suggested by Hofer and Anderson,[8] propellant supplied to the anode may be expected to be better utilized (in terms of accelerating voltage and divergence) than gas ingested through the exit plane, and contribute to increased thrust with decreasing background pressure.

Specific impulse was, to within measurement uncertainty, nearly invariant with background pressure while operating with the internal cathode. In contrast, specific impulse decreased by an average of 5.0% between the highest and lowest background pressures with the external cathode. Similar statements can be made with regard to thruster efficiency, with an average decrease of 5.6% between the highest and lowest pressures while using the external cathode.

Discharge current noise decreased with decreasing background pressure in all cases. The 400 V operating points were noisier than those at 300 V, and were less sensitive to pressure. For a given operating power and voltage, in most cases operation with the internal cathode was noisier than with the external. Fourier transforms of the discharge current time histories revealed that the bulk of the discharge current oscillations formed a prominent peak centered within the frequency range often associated with the breathing mode instability. The center frequency of these oscillations was higher at 400 V than at 300 V, and decreased with decreasing pressure in all cases. The breathing mode oscillation frequency is thought to scale inversely with the neutral transit time across the "zone of ionization,"[9] so the decrease in frequency with decreasing pressure may indicate a stretching of the ionization zone or a reduction in neutral velocity, or, more generally, an increase in the time required to replenish neutrals in the ionization zone. For a given operating condition, the breathing mode frequency was higher for the internal cathode. A similar result was reported in Ref. 8, wherein it was suggested that the ionization zone was stretched in the downstream direction when the external cathode was used due to relatively poor coupling between the cathode (located outside the separatrix) and the discharge chamber.

It is interesting to note that variations (some apparently non-linear) in thruster performance and discharge stability were observed at pressures below values that have been recommended in the literature as being acceptable for ground-test measurements of Hall thruster performance (2E-5 Torr from Ref. 10 and 3E-5 Torr from Ref. 11). A similar result was reported in Ref. 3 for the SPT-100 Hall thruster.

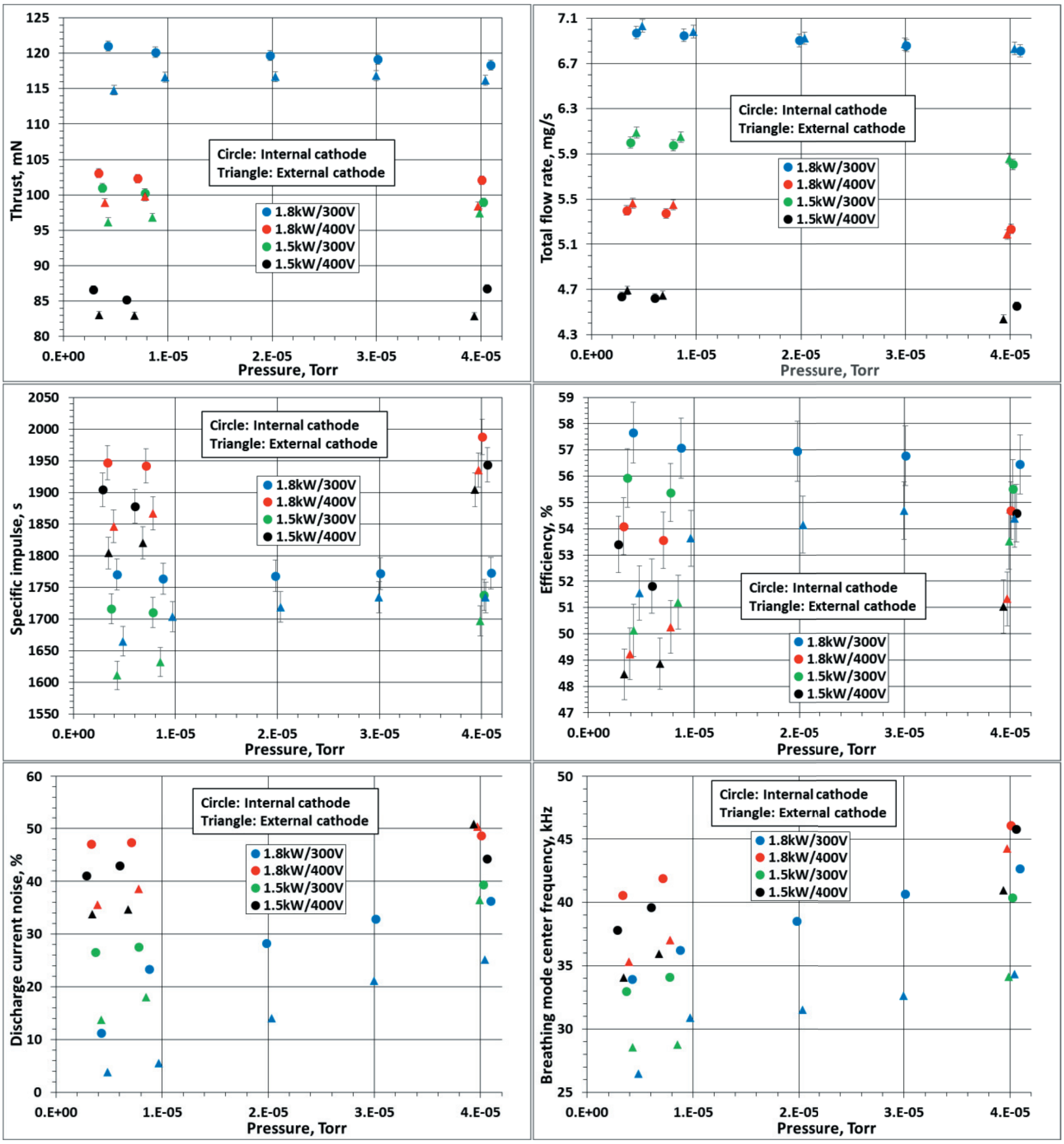

Figure 3. Performance and discharge current oscillation characteristics with 6% cathode flow fraction.

2. Effect of cathode flow fraction

Figure 4 shows the effect of cathode flow fraction on thruster performance and discharge current oscillation characteristics at the 1.8 kW, 300 V operating point for two different background pressures. The nominal 6% flow fraction was found to be approximately optimal for the external cathode. Reduction to a 3% flow fraction resulted in a substantial performance penalty, and increased discharge noise, while using the external cathode at low background pressure. Interestingly, this penalty was almost eliminated by operating at a higher background pressure (1E-5 Torr), but one that was still under the limits suggested in Refs. 10 and 11. Put another way, it is interesting to note that increasing the external cathode flow fraction from 3 to 6% had nearly the same effect as raising the background pressure from 5E-6 to 1E-5 Torr (with cathode flow fraction at 3%). Reduction to 3% flow fraction while operating the internal cathode resulted in improved performance regardless of background pressure. Other considerations, such as effects on cathode life and electromagnetic emissions, may be relevant to the decision to operate at a flow fraction of 3%.

Decreasing the cathode flow fraction had effects on discharge noise and breathing mode frequency that were similar to those observed with decreasing background pressure, presumably because both have the effect of reducing the neutral density downstream of the cathode.

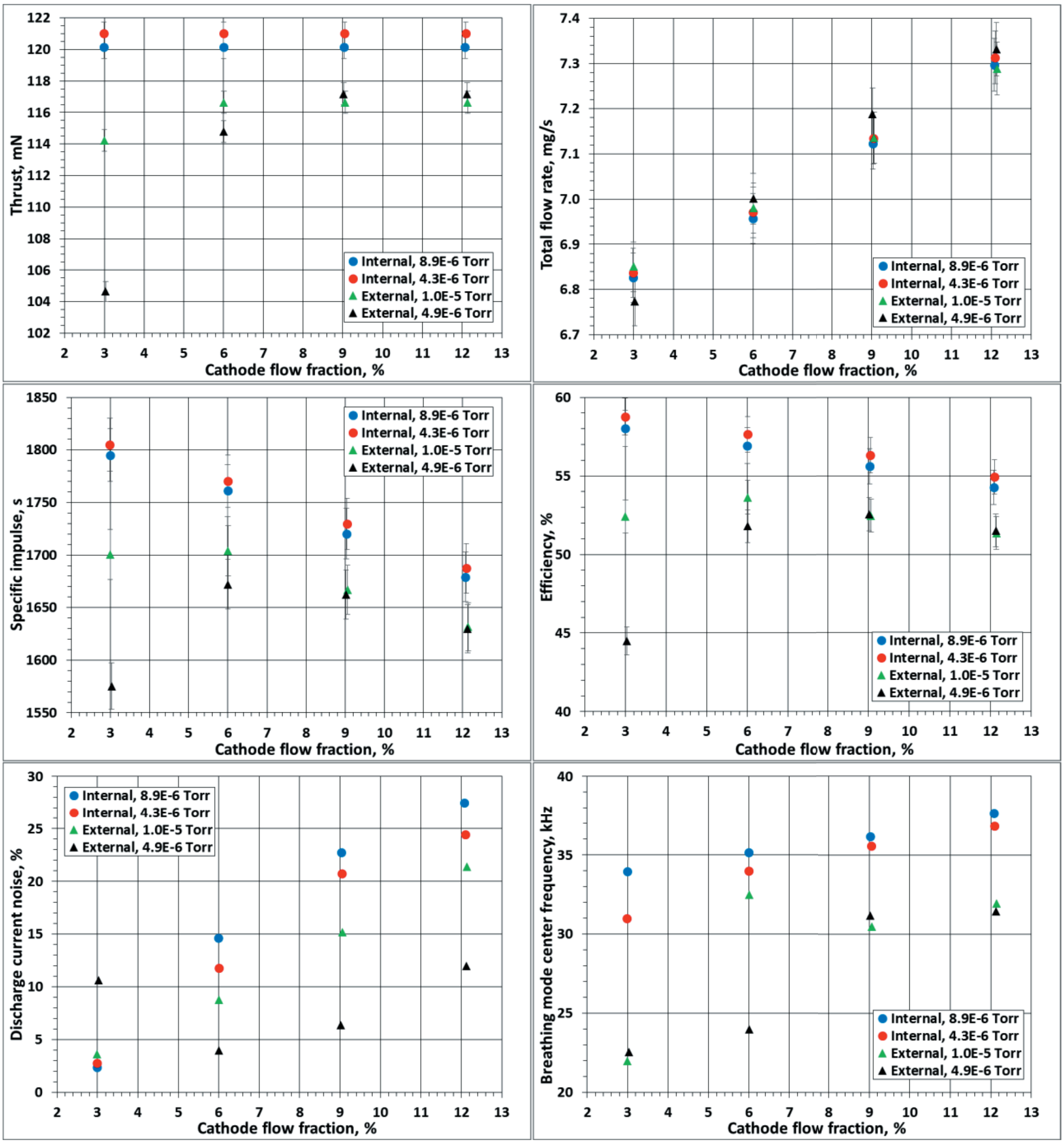

Figure 4. Effect of cathode flow fraction on thruster performance and discharge current oscillation characteristics at 1.8 kW, 300 V.

B. Plume properties

1. Potential, temperature, and density

Results from Langmuir probe measurements at 100 cm radius during operation at 1.8 kW, 300 V are shown in Fig. 5 for three different values of background pressure. Measurement uncertainties are estimated to be 0.2 V for plasma potential, 20% for electron temperature, and 30% for electron density. The measurement angular resolution was 5°. Plasma potential is presented with respect to ground for the sake of following common practice, and with respect to cathode potential. Potentials relative to the cathode are expected to be more relevant to the assessment of cathode-plume coupling and its effects on performance and plume properties. It is evident that the internal cathode coupled more efficiently to the plume, and with less sensitivity to background pressure. Reduced energy invested in driving electrons from the cathode into the plume resulted in lower electron temperatures during operation with the internal cathode. To within measurement uncertainty, electron density profiles were unaffected by cathode location. Increased electron density with increasing background pressure presumably resulted from an increasing population of slow ions produced by elastic scattering of primary ions on background neutrals, and by electron-impact ionization of background neutrals.

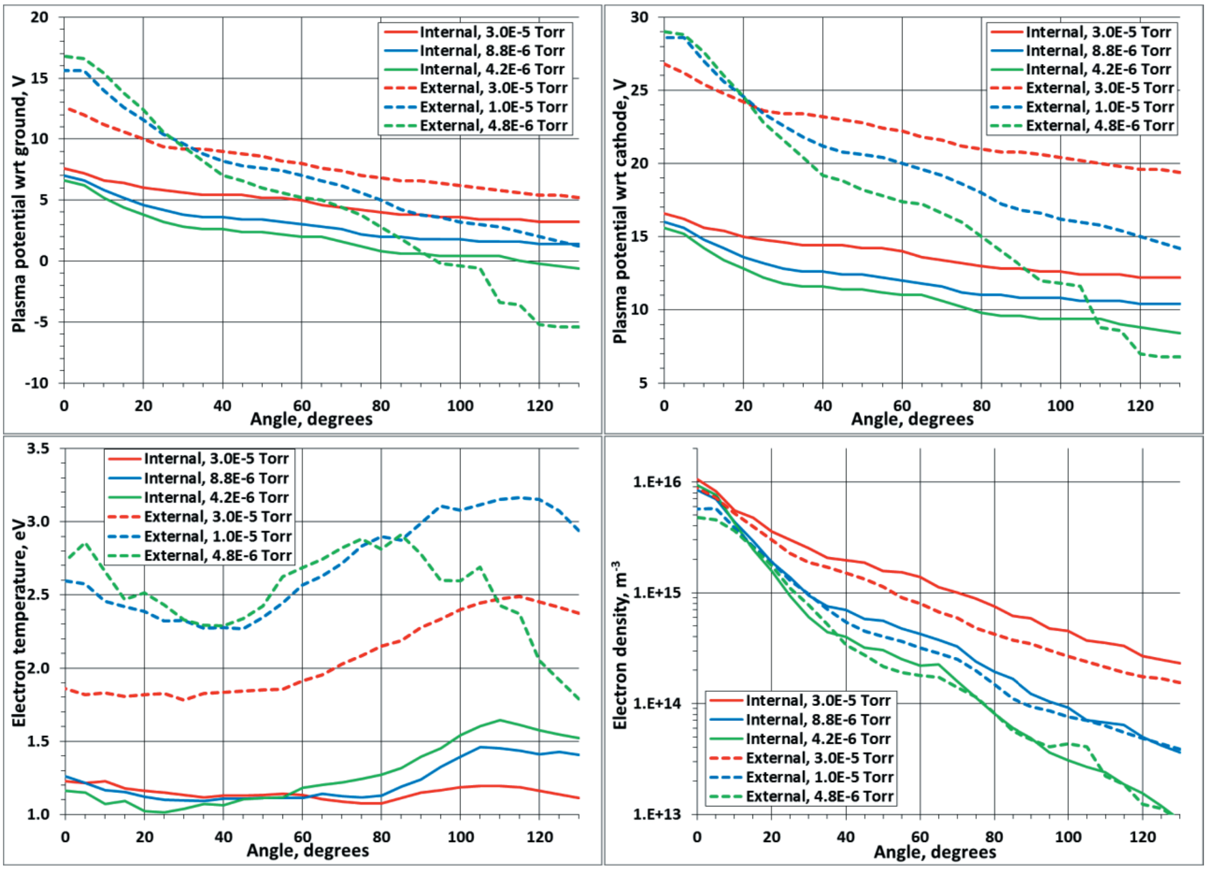

Figure 5. Langmuir probe results at 100 cm radius during operation at 1.8 kW, 300 V.

2. Ion flux

Ion flux measurements made with the RPA and Langmuir probe at a radius of 100 cm and with an angular resolution of 5° while operating at 1.8 kW, 300 V are shown in Fig. 6 for three different values of background pressure. Data from the RPA are labeled "RPA X," where X is the ion-repelling bias with respect to ground (i.e., only ions with energy-to-charge ratios greater than X were collected). Langmuir probe flux measurements are based on the extrapolation of ion current to plasma potential, as described in Section II.D.3. A notable feature is that the high-energy ion flux in the core of the plume decreased with decreasing pressure while operating with the external cathode. This result is contrary to what would be expected if elastic scattering with background neutrals were the only mechanism operating to influence the flux profile, and is evidence of increased beam divergence, i.e., the primary ion-accelerating electric field was altered by background pressure. The flux of ions with energy-to-charge ratios greater than 100 V is shown in Fig. 7 at three different background pressures. It is clear that the plume

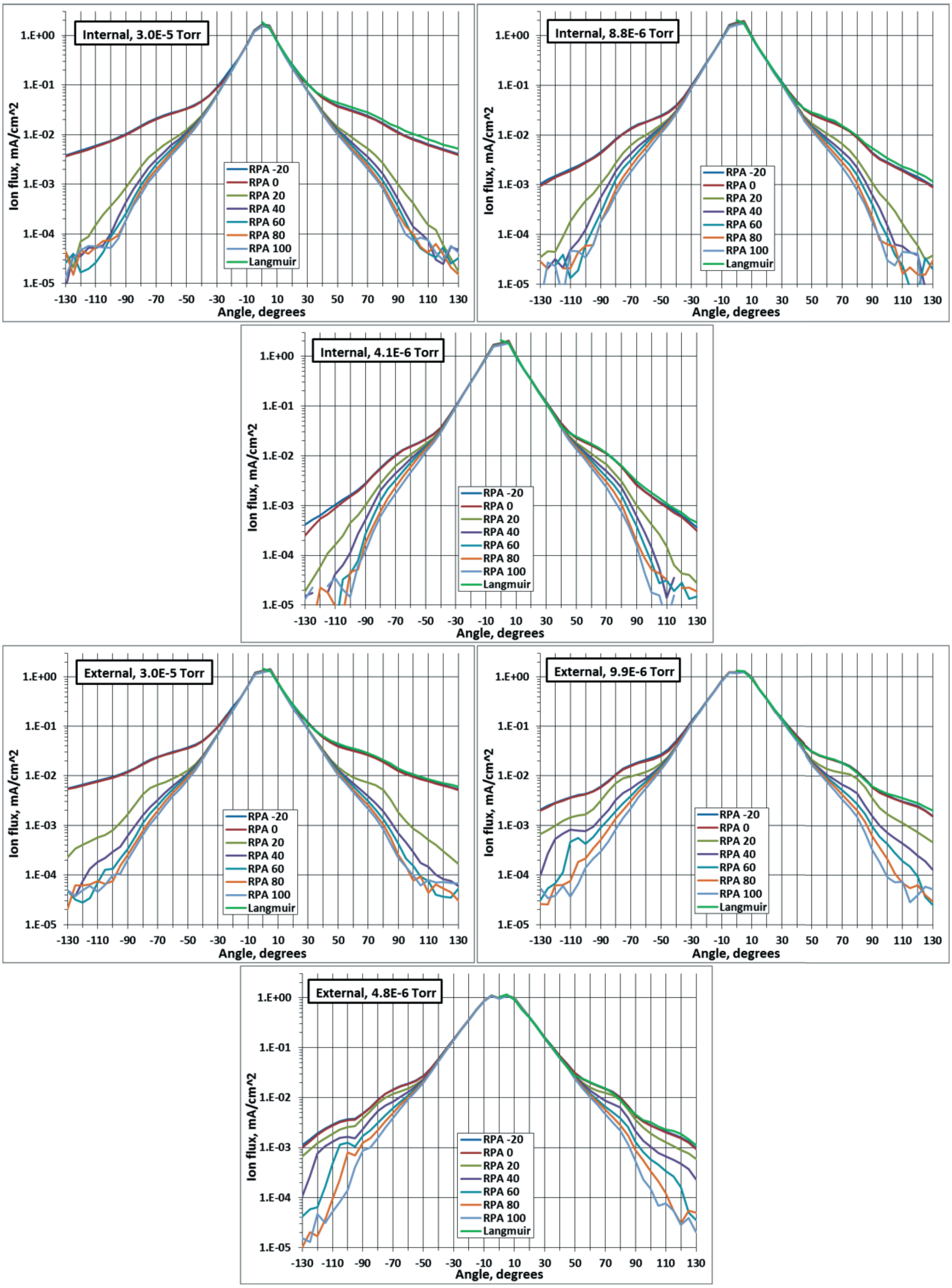

Figure 6. Ion flux at 100 cm radius during operation at 1.8 kW, 300 V.

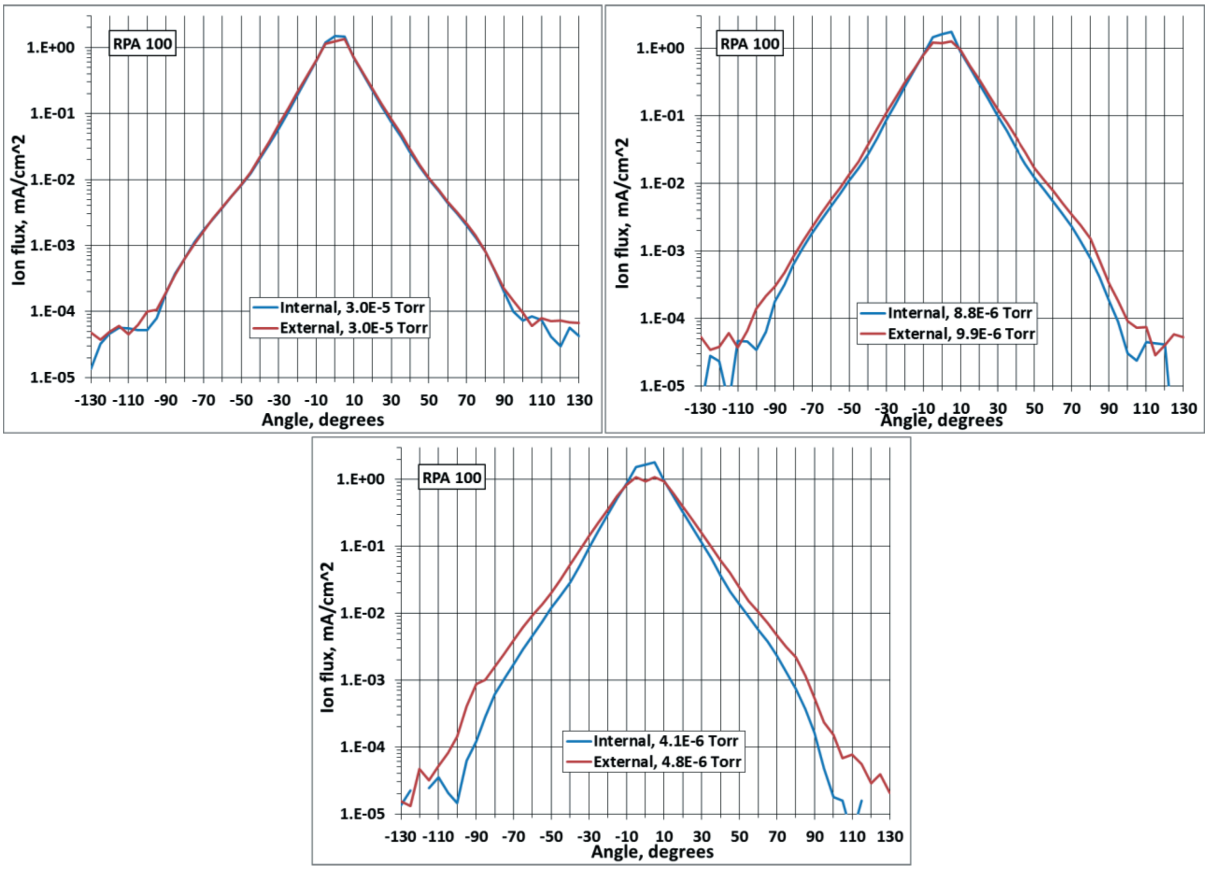

Figure 7. Effect of background pressure on plume divergence at the 1.8 kW, 300 V operating point.

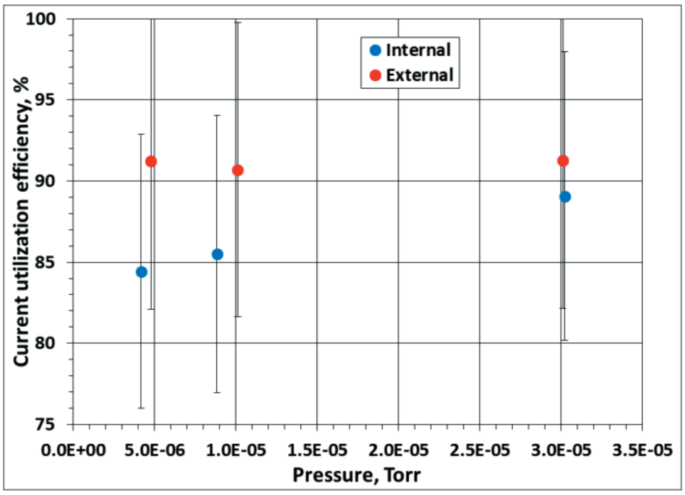

Figure 8. Current utilization efficiency at the 1.8 kW, 300 V operating point.

divergence while operating with the external cathode increased relative to that produced with the internal cathode as pressure decreased. More evidence of the effect of cathode location on plume divergence will be presented in the next section.

Figure 8 presents estimates of the current utilization efficiency η_c (ratio of plume ion current to discharge current) determined by integration of ion flux measured with the Langmuir probe while at the 1.8 kW, 300 V operating point. The Langmuir probe is well-suited to this determination because it does not discriminate against collection of slow ions produced by charge exchange reactions, and these ions need to be collected in order to properly estimate the plume ion current. Unfortunately, the Langmuir probe will also collect slow ions produced by electron-impact ionization of background neutrals, and, perhaps more significantly, there is no theory available for our probe geometry to evaluate the accuracy of a linear extrapolation of ion current to plasma potential. We have also made no attempt to correct for secondary electron emission from the probe collector. It is therefore not trivial to estimate measurement uncertainty in the determination of η_c. In Fig. 8 we have represented it as 10%, which we suspect may be an underestimate. However, since the error is expected to be mostly systematic, and in the same direction regardless of cathode choice, the conclusion that η_c was larger during operation with the external cathode than with the internal may be valid.

3. Ion energy

Ion energy distributions measured with respect to ground at a radius of 100 cm while operating at 1.8 kW, 300 V are shown in Fig. 9 for three different values of background pressure. In discussion to follow, “primary ion peak” refers to the prominent peak located at energy-to-charge ratios (E/q) just below the discharge voltage, and E/q_{max} refers to the value of E/q at the maximum of the primary ion peak (i.e., the most probable value of E/q for primary ions). At the two lowest pressures the data at 20° were distorted and the primary peak spuriously shifted to lower E/q by high current density and the resultant accumulation of space charge within the probe.

Several features of the data in Fig. 9 are noteworthy. To within the measurement uncertainty of ± 2 V, E/q_{max} was invariant with angle during operation with either cathode. As shown in Fig. 10, E/q_{max} increased slightly with decreasing pressure for both cathodes, and was, on average, 4 V higher while operating with the internal cathode than with the external. The energies of slow ions ($E/q < \sim 50$ V) were larger during operation with the external cathode, reflective of larger values of plume plasma potential, and were more strongly influenced by background pressure than while operating with the internal cathode. Increasing near-field plasma potential, while E/q_{max} remained approximately constant, is expected to result in a reduction in the net ion accelerating voltage and a corresponding reduction in thrust.

Primary ions were detected out to 90° from thruster centerline during operation with the internal cathode, and to 95° with the external. Attenuation of primary ions with increasing background pressure was expected to occur as a result of elastic collisions between ions and neutrals. At the average E/q_{max} of 282 V, the cross section for the Xe^+ + Xe symmetric charge exchange (SCX) reaction is approximately 5.4E-19 m^2.[7] Calculated values of the differential cross section for elastic scattering of 300 eV Xe^+ on Xe with and without charge exchange are presented in Ref. 12, allowing us to estimate that the total cross section for elastic scattering of primary ions is approximately 30% larger than the SCX cross section, or 7.0E-19 m^2. The data in Fig. 9 permit calculation of an effective primary ion attenuation cross section. Averaged over angles from 30° to 90°, a value of 7.1E-19 m^2 was obtained from the internal cathode data, and 1.3E-18 m^2 from the external cathode data. Variations in primary ion content with background pressure outside of the plume core can therefore be entirely attributed to plume scattering for the case of the internal cathode, but another process must be invoked in the case of the external cathode, and this is presumably that the primary ion accelerating electric field was altered by background pressure, resulting in a more divergent plume, and reduced thrust, as pressure decreased. Sommerville and King,[13] and Hofer et al.[14] have suggested that external cathode mounting, in particular outside the separatrix, enhances radial electric fields in the near-field plume, resulting in increased beam divergence relative to cathodes mounted centrally, or at least inside the separatrix.

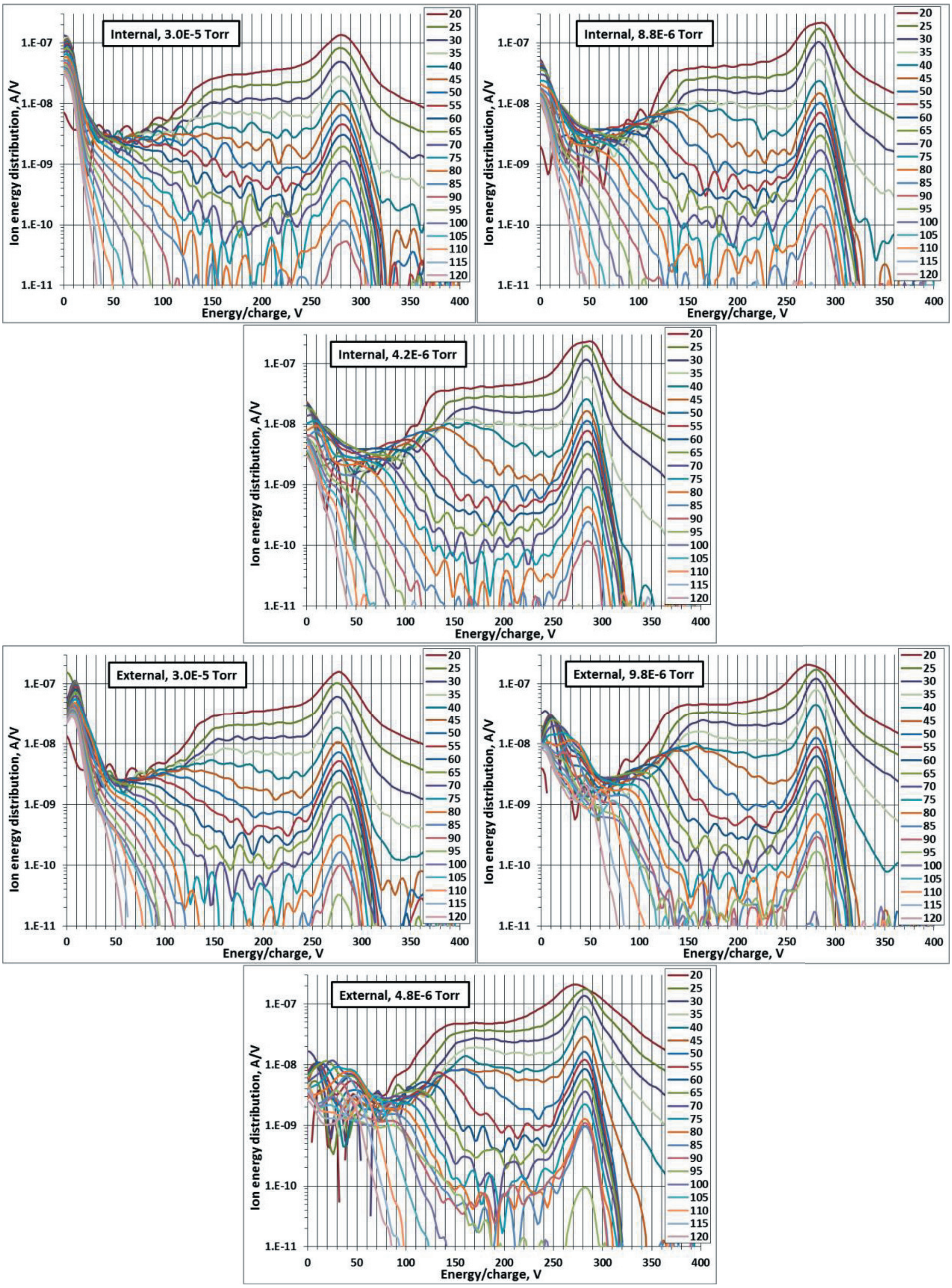

Figure 9. Ion energy distributions at 100 cm radius during operation at 1.8 kW, 300 V.

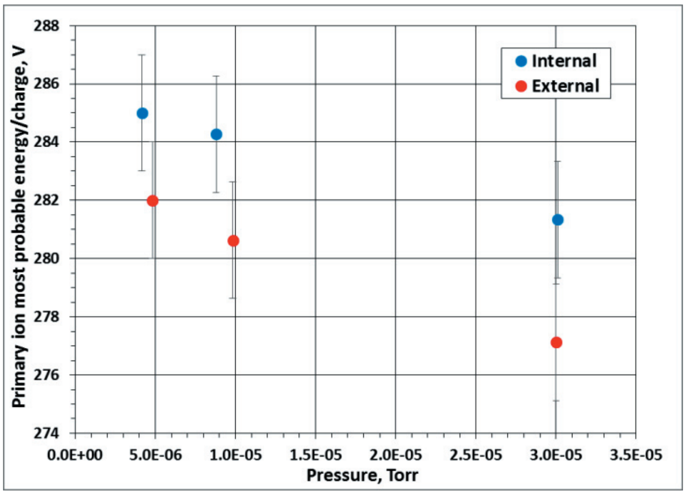

Figure 10. Energy-to-charge ratios at the primary ion peak maximum, averaged over angles.

4. Ion charge state

Ion charge state current fractions measured at a radius of 49 cm and with a measurement angular resolution of 5° while operating at 1.8 kW, 300 V are shown in Fig. 11 for three different values of background pressure. Included on the plots are current fractions for Xe^{+} (j^{+}/j), Xe^{2+} (j^{2+}/j), Xe^{3+} (j^{3+}/j) and Xe^{4+} (j^{4+}/j). Measurement uncertainties for the current fractions were estimated to be 2% for Xe^{+}, 10% for Xe^{2+}, 20% for Xe^{3+}, and 50% for Xe^{4+}. Valid data were obtained over more limited angular ranges for Xe^{3+} and Xe^{4+} than for Xe^{+} and Xe^{2+}. Data were not obtained at angles less than 20° because of excessive broadening and overlap of the peaks in the ExB probe spectrum, presumably caused by space charge buildup within the probe. During operation with the internal cathode at all three background pressures, Xe^{+} primary ions were detected out to a maximum of 90° from thruster centerline. Xe^{+} primary ions were detected out to 90° at 3.0E-5 Torr, and then to 100° at 9.9E-6 and 4.8E-6 Torr while operating with the external cathode. Xe^{3+} and Xe^{4+} current fractions decreased monotonically with angle away from thruster centerline, while the Xe^{2+} fraction was maximized at approximately 40° ± 5°, and Xe^{+} reached a minimum at approximately 35° ± 5°, all regardless of cathode location.

Charge state current fractions were affected by background pressure, with a decrease in multi-charged ions as pressure decreased. This is clearly evident from Fig. 12, which shows total current fractions obtained by integration of the data in Fig. 11. (We remind the reader that these data have been corrected with regard to variation in the charge exchange cross section with charge state, as described in Section II.D.5.) To within measurement uncertainty, total current fractions were independent of cathode location. Decreased multi-charged ion content could be indicative of decreased electron temperature in the thruster discharge. Decreased multi-charged ion content in a Hall thruster plume with decreasing background pressure has also been reported in Refs. 15 and 16, and should result in increased thrust.[17]

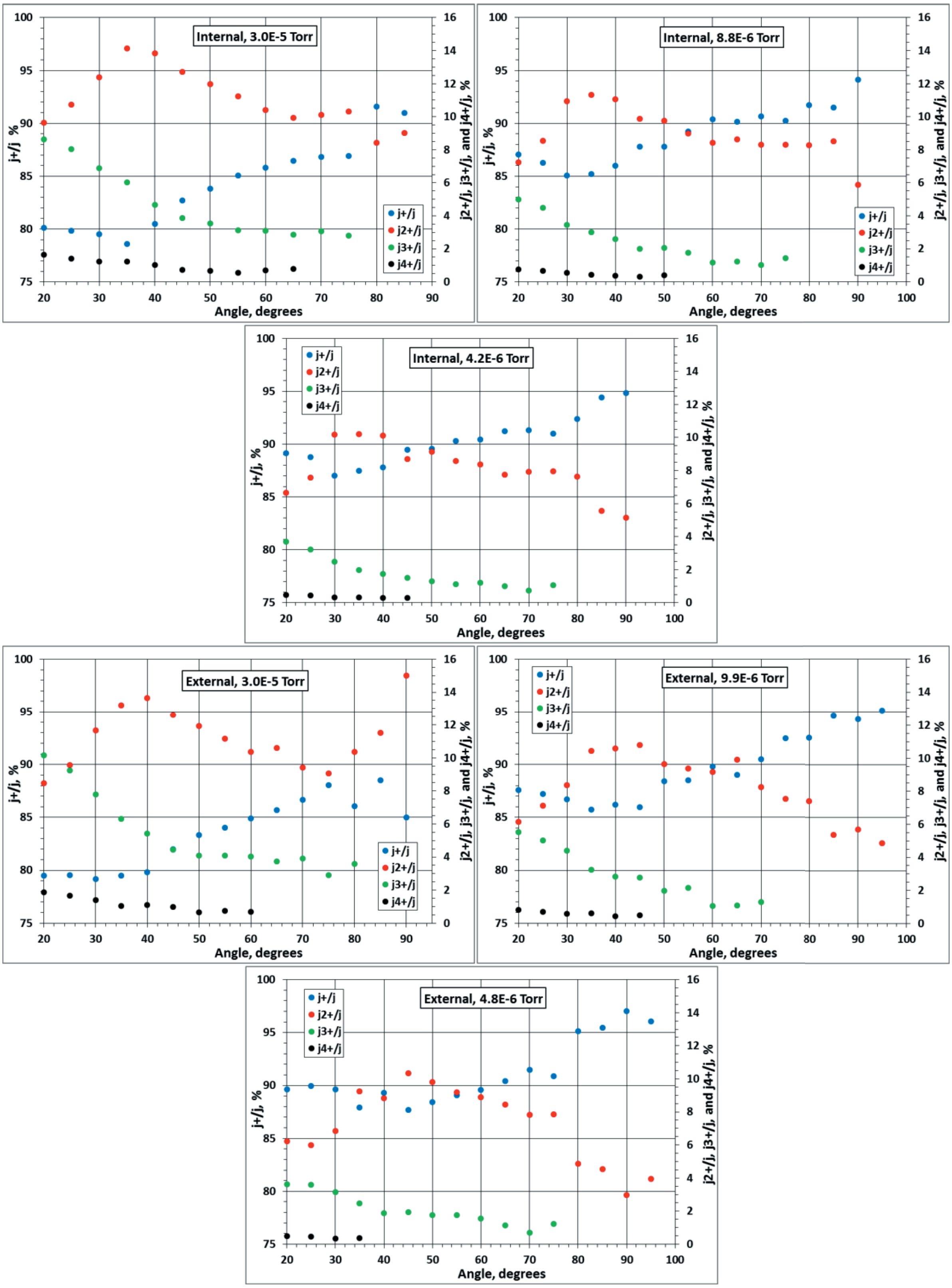

Figure 11. Ion charge state distributions at 49 cm radius during operation at 1.8 kW, 300 V.

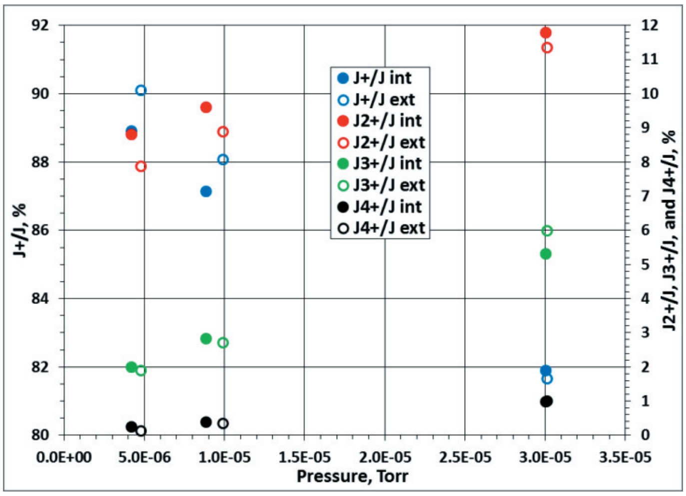

Figure 12. Total current fractions.

IV. Conclusion

There are three main conclusions from this work. The first is that the BHT-1500 Hall thruster is a mature device with world-class performance in its power range. The second is that mounting the cathode on thruster centerline confers a number of advantages relative to external mounting. These include increased performance (thrust, specific impulse, and efficiency), reduced sensitivity of performance to cathode flow rate, more efficient cathode-plume coupling, and reduced sensitivity of the aforementioned, as well as plume divergence, to vacuum facility background pressure. These characteristics have been reported by others in the Hall thruster literature, and discussed relative to the phenomenology of electron cross-field mobility in the near-field plume.[8,13-15] However, the third conclusion from this work is that background pressure produces other effects on thruster operation that appear to be largely independent of cathode location, and which continue to present themselves at pressures below those recommended in the literature for high-fidelity Hall thruster performance testing. These include variations in the discharge oscillation amplitude and frequency, the most-probable primary ion energy-to-charge ratio, the fraction of multi-charged ions, and the total xenon flow rate. As discussed in Ref. 3, while operating at typical vacuum chamber background pressures (~ 1-3E-5 Torr), background neutral densities can be comparable to neutral densities near the exit plane of a Hall thruster, implying that background neutrals may play a significant role in ionization and conduction in that region.

References

[1]Pote, B. and Tedrake, R., "Performance of a High Specific Impulse Hall Thruster," IEPC 2001-35.

[2]Szabo, J.J. and Azziz, Y., "Characterization of a High Specific Impulse Xenon Hall Effect Thruster," IEPC 2005-324.

[3]Diamant, K.D., Liang, R., and Corey, R.L., "The Effect of Background Pressure on SPT-100 Hall Thruster Performance," AIAA 2014-3710.

[4]Pollard, J.E., Diamant, K.D., Crofton, M.W., Patterson, M.J., and Soulas, G.C., "Spatially-Resolved Beam Current and Charge-State Distributions for the NEXT Ion Engine," AIAA 2010-6779.

[5]Reid, B.M., Shastry, R., and Gallimore, A.D., "Angularly-Resolved ExB Probe Spectra in the Plume of a 6-kW Hall Thruster," AIAA 2008-5287, July 2008.

[6]Shastry, R., Hofer, R.R., Reid, B.M., and Gallimore, A.D., "Method for Analyzing ExB Probe Spectra from Hall Thruster Plumes," Review of Scientific Instruments, 80, 063502 (2009).

[7]Miller, J.S., Pullins, S.H., Levandier, D.J., Chiu, Y., and Dressler, R.A., "Xenon Charge Exchange Cross Sections for Electrostatic Thruster Models," Journal of Applied Physics, Vol. 91, No. 3, February 2002, pp. 984-991.

[8]Hofer, R.R. and Anderson, J.R., "Finite Pressure Effects in Magnetically Shielded Hall Thrusters," AIAA 2014-3709.

[9]Choueiri, E.Y., "Plasma Oscillations in Hall Thrusters," Physics of Plasmas, Vol. 8, No. 4, April 2001, pp. 1411-1426.

[10]Biagioni, L., Kim, V., Nicolini, D., Semenkin, A.V., and Wallace, N.C., "Basic Issues in Electric Propulsion Testing and the Need for International Standards," IEPC 2003-230.

[11]Dankanich, J.W., Walker, M., Swiatek, M.W., and Yim, J.T., "Recommended Practice for Pressure Measurements and Calculation of Effective Pumping Speeds during Electric Propulsion Testing," IEPC 2013-358.

[12]Boyd, I.D. and Dressler, R.A., "Far Field Modeling of the Plasma Plume of a Hall Thruster," Journal of Applied Physics, Vol. 92, No. 4, August 2002, pp. 1764-1774.

[13]Sommerville, J.D. and King, L.B., "Hall-Effect Thruster-Cathode Coupling, Part II: Ion Beam and Near-Field Plume," Journal of Propulsion and Power, Vol. 27, No. 4, July-August 2011.

[14]Hofer, R.R., Johnson, L.K., and Goebel, D.M., "Effects of Internally Mounted Cathodes on Hall Thruster Plume Properties," IEEE Transactions on Plasma Science, Vol. 36, No. 5, October 2008, pp. 2004-2014.

[15]Huang, W., Kamhawi, H., and Haag, T., "Effect of Background Pressure on the Performance and Plume of the HiVHAc Hall Thruster," IEPC 2013-058.

[16]Diamant, K.D., Spektor, R., Beiting, E.J., Young, J.A., and Curtiss, T.J., "The Effects of Background Pressure on Hall Thruster Operation," AIAA 2012-3735.

[17]Goebel, D.M. and Katz, I., Fundamentals of Electric Propulsion, Ion and Hall Thrusters, John Wiley and Sons, 2008, p. 24.